Title	Transmission power variance constrained power allocation for iterative frequency domain multiuser SIMO detector
Author(s)	Tervo, Valtteri; Tolli, A.; Karjalainen, J.; Matsumoto, Tad
Citation	2014 IEEE International Conference on Acoustics, Speech and Signal Processing (ICASSP): 3493-3497
Issue Date	2014
Type	Conference Paper
Text version	author
URL	http://hdl.handle.net/10119/12954
Rights	This is the author's version of the work. Copyright (C) 2014 IEEE. 2014 IEEE International Conference on Acoustics, Speech and Signal Processing (ICASSP), 2014, 3493-3497. Personal use of this material is permitted. Permission from IEEE must be obtained for all other uses, in any current or future media, including reprinting/republishing this material for advertising or promotional purposes, creating new collective works, for resale or redistribution to servers or lists, or reuse of any copyrighted component of this work in other works.
Description	

Transmission Power Variance Constrained Power Allocation for Iterative Frequency Domain Multiuser SIMO Detector

Valtteri Tervo*+, A Tölli*, J. Karjalainen†, Tad Matsumoto*+

{wade, atolli, matumoto}@ee.oulu.fi, juha.karjalainen@renesasmobile.com

*Centre for Wireless Communications, University of Oulu, P.O. Box 4500, 90014 University of Oulu, Finland.
+Japan Advanced Institute of Science and Technology, 1-1 Asahi-Dai, Nomi, Ishikawa, 923-1292 Japan.
†Renesas Mobile Europe Oy, Elektroniikkatie 13, 90590 OULU, Finland

Abstract—**Transmission power variance constrained power allocation in single carrier multiuser (MU) single-input multiple-output (SIMO) systems with iterative frequency domain (FD) soft cancelation (SC) minimum mean squared error (MMSE) equalization is considered in this paper. It is known in the literature that peak to average power ratio (PAPR) at the transmitter can be reduced by reducing the variance of the transmit power. In this paper, we derive a power variance constraint to statistically control the PAPR. This constrained is plugged in to a convergence constrained power allocation (CCPA) problem and a successive convex approximation (SCA) is derived via geometric program (GP). Numerical results are presented in the form of complementary cumulative distribution functions (CCDFs) to demonstrate the effectiveness of the proposed method.**

I. INTRODUCTION

The use of frequency division multiplexing via discrete Fourier transform (DFT) causes a high peak-to-average power ratio (PAPR), which necessitates expensive and power-inefficient radio-frequency (RF) components at the transmitter. Recent work on minimizing the PAPR in single carrier frequency division multiple access (FDMA) [1] transmission can be found in [2]–[4], where they propose different precoding methods for PAPR reduction. However, these methods do not take into account the transmit power allocation, the channel nor the receiver. PAPR-aware large-scale multiuser (MU) multiple-input multiple-output (MIMO) orthogonal frequency division multiplexing (OFDM) downlink is investigated in [5] where they assume the massive degrees-of-freedom available to achieve low PAPR.

To exploit the full merit of iterative receiver, the convergence properties of an iterative receiver needs to be taken into account at a transmitter side. This issue has been thoroughly investigated in [6] where the power allocation to different channels is optimized subject to a quality of service (QoS) constraint taking into account the convergence properties of iterative frequncy domain (FD) soft cancelation (SC) minimum mean squared error (MMSE) MIMO receiver. The convergence properties were examined by using extrinsic information transfer (EXIT) charts [7]. The concept in [6] has been extended for MU systems in [8], [9]. In this paper, we will introduce a power variance constraint for the convergence constrained power allocation (CCPA) problem presented in [9]. In other words, we will minimize the total transmit power in a cell with multiple users while guaranteeing the desired QoS in terms of bit error probability (BEP) and keeping the transmit power variance always below the desired value.

The main contributions of this paper are summarized as follows: The expected power variance of the transmitted waveform is derived
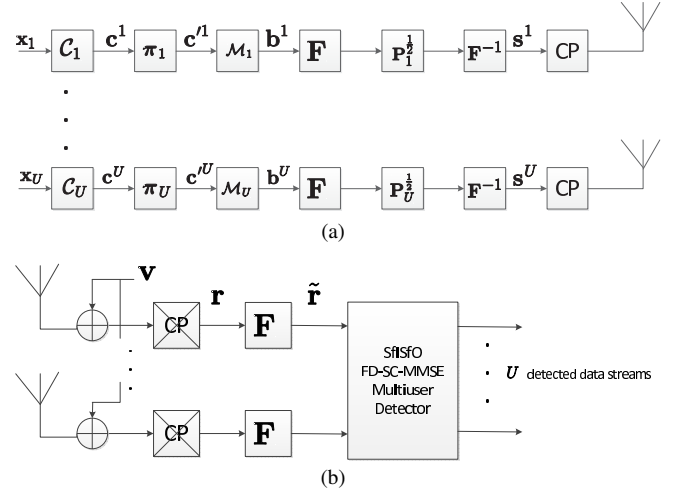
Fig. 1. The block diagram of (a) the transmitter side (b) the receiver side of the system model.

as a function of power allocation. The variance constraint is derived and a local convex approximation of the constraint is formulated via geometric program (GP) [10]. The constraint is plugged in to a CCPA problem and solved by successive convex approximation (SCA) algorithm [11].

II. SYSTEM MODEL

Consider a single carrier uplink transmission with U single-antenna users and a base station with N_R antennas as depicted in Fig. 1. Each user's data stream is encoded by forward error correction code (FEC) $\mathcal{C}_u$, $u = 1, 2, \ldots, U$. The encoded bits are bit interleaved and mapped onto a 2^{N_Q}-ary complex symbol, where N_Q denotes the number of bits per modulation symbol. After the modulation, each user's data stream is transformed into the frequency domain by performing the discrete Fourier transform (DFT) and multiplied with its associated power allocation matrix. Finally, before transmission, each user's data stream is transformed into the time domain by the inverse DFT (IDFT) and a cyclic prefix is added to mitigate inter block interference (IBI).

At the receiver side, after the cyclic prefix removal, the signal can be expressed as

$$\mathbf{r} = \mathbf{H}_u \mathbf{F}^{-1} \mathbf{P}_u^{\frac{1}{2}} \mathbf{F} \mathbf{b}^u + \sum_{\substack{y=1 \\ y \neq u}}^{U} \mathbf{H}_y \mathbf{F}^{-1} \mathbf{P}_y^{\frac{1}{2}} \mathbf{F} \mathbf{b}^y + \mathbf{v}, \qquad (1)$$

where $\mathbf{H}_u = [\mathbf{H}_u^1, \mathbf{H}_u^2, \ldots, \mathbf{H}_u^{N_R}]^{\mathrm{T}} \in \mathbb{C}^{N_R N_F \times N_F}$ is the space-time channel matrix for user u and $\mathbf{H}_u^r =$
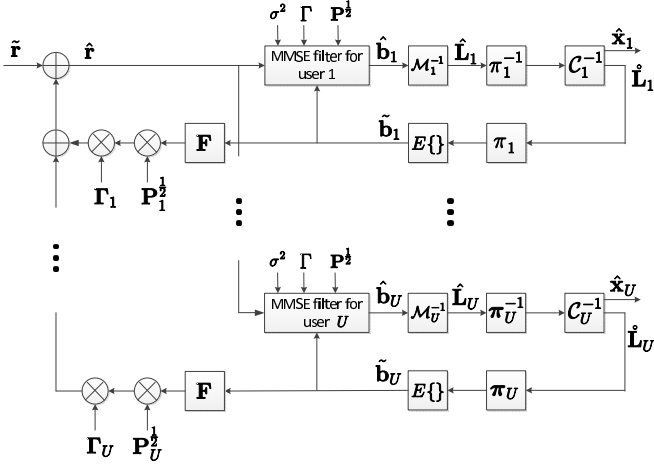
Fig. 2. The block diagram of FD-SC-MMSE turbo equalizer.

$\text{circ}\{[h_{u,1}^r, h_{u,2}^r, \ldots, h_{u,N_L}^r, \mathbf{0}_{1 \times N_F - N_L}]^T\} \in \mathbb{C}^{N_F \times N_F}$ is the time domain circulant channel matrix for user u at the receive antenna r. The operator $\text{circ}\{\}$ generates matrix that has a circulant structure of its argument vector and N_L denotes the length of the channel impulse response. $\mathbf{F} \in \mathbb{C}^{N_F \times N_F}$ denotes the DFT matrix with elements $f_{m,l} = \frac{1}{\sqrt{N_F}} \exp(i2\pi(m-1)(l-1)/N_F)$. $\mathbf{P} \in \mathbb{R}^{UN_F \times UN_F}$ is the power allocation matrix denoted as $\mathbf{P} = \text{diag}(\mathbf{P}_1, \mathbf{P}_2, \ldots, \mathbf{P}_U)$ with $\mathbf{P}_u = \text{diag}([P_{u,1}, P_{u,2}, \ldots, P_{u,N_F}]^T) \in \mathbb{R}^{N_F \times N_F}$, $u = 1, 2, \ldots, U$, and $\mathbf{b} = [\mathbf{b}^{1^T}, \mathbf{b}^{2^T}, \ldots, \mathbf{b}^{U^T}]^T$. $\mathbf{b}^u \in \mathbb{C}^{N_F}$, $u = 1, 2, \ldots, U$, is the modulated complex data vector for the uth user and $\mathbf{v} \in \mathbb{C}^{N_F}$ is white additive independent identically distributed (i.i.d.) Gaussian noise vector with variance σ_v^2.

III. PROBLEM FORMULATION

The block diagram of the FD-SC-MMSE turbo equalizer is depicted in Fig. 2. The frequency domain signal after the soft cancelation can be written as

$$\hat{\mathbf{r}} = \tilde{\mathbf{r}} - \mathbf{\Gamma}\mathbf{P}^{\frac{1}{2}}\mathbf{F}_U\tilde{\mathbf{b}}, \tag{2}$$

where $\tilde{\mathbf{b}} = [\tilde{\mathbf{b}}^{1^T}, \tilde{\mathbf{b}}^{2^T}, \ldots, \tilde{\mathbf{b}}^{U^T}]^T \in \mathbb{C}^{UN_F}$ are the soft symbol estimates of the modulated complex symbols and $\mathbf{F}_U = \mathbf{I}_U \otimes \mathbf{F} \in \mathbb{C}^{UN_F \times UN_F}$. $\mathbf{I}_U$ denotes the $U \times U$ identity matrix and $\otimes$ is the Kronecker product. $\mathbf{\Gamma} = [\mathbf{\Gamma}_1, \mathbf{\Gamma}_2, \ldots, \mathbf{\Gamma}_U] \in \mathbb{C}^{N_R N_F \times UN_F}$ and $\mathbf{\Gamma}_u = \text{bdiag}\{\mathbf{\Gamma}_{u,1}, \mathbf{\Gamma}_{u,2}, \ldots, \mathbf{\Gamma}_{u,N_F}\} \in \mathbb{C}^{N_R N_F \times N_F}$ is the space-frequency channel matrix for user u expressed as

$$\mathbf{\Gamma}_u = \mathbf{F}_{N_R}\mathbf{H}_u\mathbf{F}^{-1}. \tag{3}$$

$\mathbf{\Gamma}_{u,m} \in \mathbb{C}^{N_R \times N_R}$ is the diagonal channel matrix for m^{th} frequency bin of uth user and $\text{bdiag}\{\cdot\}$ generates block diagonal matrix of its arguments. $\hat{\mathbf{L}}_u$ and $\mathring{\mathbf{L}}_u$ in Fig. 2 denote the log-likelihood ratios (LLRs) provided by the equalizer and the channel decoder of user u, respectively, and $\hat{\mathbf{x}}_u$ denotes the estimate of $\mathbf{x}_u$.

A. Convergence Constraint

The convergence constraint can be expressed as LLR variance constraint as [6], [8], [9], [12]

$$\hat{\sigma}_{u,k}^2 \geq \mathring{\sigma}_{u,k}^2, \forall u = 1, 2 \ldots, U, \forall k = 1, 2, \ldots, K. \tag{4}$$

where $\hat{\sigma}_{u,k}^2$ and $\mathring{\sigma}_{u,k}^2$ is the variance of the LLRs at the output of the equalizer and at the input of the decoder, respectively, for u^{th} user at the k sample point in the EXIT chart. When Gray-mapped quadrature

phase shift keying (QPSK) modulation is used, the variance of the LLRs at the output of the equalizer can be expressed as [6, Eq. (17)]

$$\hat{\sigma}_{u,k}^2 = \frac{4\zeta_{u,k}}{1 - \zeta_{u,k}\bar{\Delta}_{u,k}}. \tag{5}$$

The idea is that we choose K MI points from the $U+1$-dimensional EXIT chart of the equalizer and the decoders of all the users. The K points are chosen such that all the decoder's outputs are equal, i.e., the points lie on the line from the origin to the convergence point. This approach is referred as diagonal sampling [9]. These MI points are then mapped to LLR variances yielding a sequence $\mathring{\sigma}_{u,1}^2, \mathring{\sigma}_{u,2}^2, \ldots, \mathring{\sigma}_{u,K}^2$. $\zeta_{u,k}$ in (5) is called as the effective SINR of the prior symbol estimates and is given by [9]

$$\zeta_{u,k} = \frac{1}{N_F}\sum_{m=1}^{N_F} \frac{P_{u,m}|\boldsymbol{\omega}_{u,m}^{k}{}^{\text{H}}\boldsymbol{\gamma}_{u,m}|^2}{\sum_{l=1}^{U} P_{l,m}|\boldsymbol{\omega}_{u,m}^{k}{}^{\text{H}}\boldsymbol{\gamma}_{l,m}|^2\bar{\Delta}_{u,k} + ||\boldsymbol{\omega}_{u,m}^{k}{}^{\text{H}}||^2\sigma_v^2}, \tag{6}$$

where $\boldsymbol{\gamma}_{u,m} \in \mathbb{C}^{N_R}$ consists of the diagonal elements of $\mathbf{\Gamma}_{u,m}$, i.e., $\boldsymbol{\gamma}_{u,m}$ is the channel vector for m^{th} frequency bin of user u. $\boldsymbol{\omega}_{u,m}^{k}{}^{\text{H}} \in \mathbb{C}^{N_R}$ is the receive beamforming vector for m^{th} frequency bin of user u at MI index k and it can be optimally calculated as [13]

$$\boldsymbol{\omega}_{u,m}^{k}{}^{\text{H}} = (\sum_{l=1}^{U} P_{l,m}\boldsymbol{\gamma}_{l,m}\boldsymbol{\gamma}_{l,m}^{\text{H}}\bar{\Delta}_{l,k} + \sigma_v^2\mathbf{I}_{N_R})^{-1}\boldsymbol{\gamma}_{u,m}P_{u,m}^{\frac{1}{2}}. \tag{7}$$

$\bar{\Delta}_{u,k} \in \mathbb{R}$ is the average residual interference of the soft symbol estimates and is given by

$$\bar{\Delta}_{u,k} = \text{avg}\{\mathbf{1}_{N_F} - \ddot{\mathbf{b}}^u\}, \tag{8}$$

where $\ddot{\mathbf{b}}^u = [|\tilde{b}_1^u|^2, |\tilde{b}_2^u|^2, \ldots, |\tilde{b}_{N_F}^u|^2]^T \in \mathbb{C}^{N_F}$. The soft symbol estimate $\tilde{b}_n^u$ is calculated as

$$\tilde{b}_n^u = E\{b_n^u\} = \sum_{b_i \in \mathfrak{B}} b_i \Pr(b_n^u = b_i), \tag{9}$$

where $\mathfrak{B}$ is the modulation symbol alphabet, and the symbol *a priori* probability can be calculated by

$$\Pr(b_n^u = b_i) = \prod_{q=1}^{N_Q} \Pr(c_{n,q}^u = z_{i,q})$$
$$= \left(\frac{1}{2}\right)^{N_Q} \prod_{q=1}^{N_Q}(1 - \bar{z}_{i,q}\tanh(\lambda_{n,q}^u/2)), \tag{10}$$

with $\bar{z}_{i,q} = 2z_{i,q} - 1$ and $\mathbf{z}_i = [z_{i,1}, z_{i,2}, \ldots, z_{i,N_Q}]^T$ is the binary representation of the symbol b_i, depending on the modulation mapping. $\lambda_{n,q}^u$ is the *a priori* LLR of the bit $c_{n,q}^u$, provided by the decoder of user u. Plugging (5) into (4), the convergence constraint can be written as [9]

$$\frac{1}{N_F}\sum_{m=1}^{N_F} \frac{P_{u,m}|\boldsymbol{\omega}_{u,m}^{k}{}^{\text{H}}\boldsymbol{\gamma}_{u,m}|^2}{\sum_{l=1}^{U} P_{l,m}|\boldsymbol{\omega}_{u,m}^{k}{}^{\text{H}}\boldsymbol{\gamma}_{l,m}|^2\bar{\Delta}_{l,k} + ||\boldsymbol{\omega}_{u,m}^{k}{}^{\text{H}}||^2\sigma_v^2} \tag{11}$$
$$\geq \xi_{u,k}, \forall u = 1, 2 \ldots, U, \forall k = 1, 2, \ldots, K, \tag{12}$$

where

$$\xi_{u,k} = \frac{(\mathring{\sigma}_{u,k})^2}{4 + (\mathring{\sigma}_{u,k})^2\bar{\Delta}_{u,k}} \tag{13}$$

is constant.

B. Power Variance Constraint

Because the PAPR is derived similarly for all the users, the user index is omitted in this section. Let $\mathbf{G} = \mathbf{F}^{-1}\mathbf{P}^{\frac{1}{2}}\mathbf{F}$. The entry (m,n) of $\mathbf{G}$ is obtained as

$$g_{m,n} = \frac{1}{N_F}\sum_{l=1}^{N_F}\sqrt{P_l}e^{\frac{j2\pi(l-1)(n-m)}{N_F}}. \tag{14}$$

Let s_m be the mth output of the transmitted waveform after the IFFT as depicted in Fig. 1(a). Assuming $|b_n| = 1$, $\forall n$ and $\mathbb{E}\{b_p b_q^*\} = 0$, $\forall p \neq q$, where b_q^* denotes the complex conjugate of b_q, the average of the transmit power can be calculated as

$$\mu = \text{avg}[|s_m|^2] = \frac{1}{N_F}\sum_{m=1}^{N_F}\mathbb{E}\left\{[|s_m|^2]\right\}$$
$$= \frac{1}{N_F}\sum_{l=1}^{N_F}P_l. \tag{15}$$

The variance of the output power is given by

$$\Sigma^2(\mathbf{P}) = \frac{1}{N_F}\sum_{k=1}^{N_F}(\mathbb{E}[|s_k|^4] - \mu^2)$$
$$= \frac{1}{N_F}\sum_{k=1}^{N_F}[2(\sum_{m=1}^{N_F}|g_{k,m}|^2)^2 - \sum_{m=1}^{N_F}|g_{k,m}|^4] - \mu^2. \tag{16}$$

The first term reduces to

$$\frac{1}{N_F}\sum_{k=1}^{N_F}(\sum_{m=1}^{N_F}|g_{k,m}|^2)^2 = \mu^2. \tag{17}$$

The second term can be expressed as a function of power allocation as

$$\frac{1}{N_F}\sum_{k=1}^{N_F}\sum_{m=1}^{N_F}|g_{k,m}|^4$$
$$= \frac{\mu^2}{N_F} + \frac{1}{N_F^3}\sum_{p,q \in \mathcal{S}_1}P_pP_q + \frac{1}{N_F^3}\sum_{p,q,r,s \in \mathcal{S}_2}\sqrt{P_pP_qP_rP_s}, \tag{18}$$

where $\mathcal{S}_1 = \{p,q \in \{1,2,\dots,N_F\} : p \neq q, p - q = \pm N_F/2\}$ and $\mathcal{S}_2 = \{p,q,r,s \in \{1,2,\dots,N_F\} : p \neq q, r \neq s, (p,q) \neq (r,s), s - r \in \{p - q, N_F + p - q, -N_F + p - q\}\}$. Substituting (17) and (18) to (16) we get

$$\Sigma^2(\mathbf{P}) = \frac{N_F - 1}{N_F^3}(\sum_{l=1}^{N_F}P_l)^2 - \frac{1}{N_F^3}\sum_{p,q \in \mathcal{S}_1}P_pP_q -$$
$$\frac{1}{N_F^3}\sum_{p,q,r,s \in \mathcal{S}_2}\sqrt{P_pP_qP_rP_s}. \tag{19}$$

The objective is to control the variance of the normalized power. This constraint is written as

$$\frac{\Sigma^2(\mathbf{P})}{(\sum_{l=1}^{N_F}P_l)^2} \leq \sigma_s^2, \tag{20}$$

where $\sigma_s^2 \in \mathbb{R}^+$ is the maximum power variance. Plugging (19) to (20) the constraint can be written as

$$(N_F - 1)(\sum_{l=1}^{N_F}P_l)^2 \leq \sum_{p,q \in \mathcal{S}_1}P_pP_q +$$
$$\sum_{p,q,r,s \in \mathcal{S}_2}\sqrt{P_pP_qP_rP_s} + (\sum_{l=1}^{N_F}P_l)^2\sigma_s^2 N_F^3. \tag{21}$$

C. Successive Convex Approximation

Our objective is to minimize the total transmitted power with the constraints (11) and (21). Hence, the objective is linear but both (11) and (21), are nonconvex constraints. However, we can derive a successive convex approximation for the problem via GP using the inequality [9]

$$\sum_{m=1}^{N_F}t_m \geq \prod_{m=1}^{N_F}(\frac{t_m}{\Phi_m})^{\Phi_m}, \tag{24}$$

where $\Phi_m = \frac{\hat{t}_m}{\sum_{n=1}^{N_F}\hat{t}_n}$, $\hat{t}_m > 0$, and $t_m > 0$, $m = 1,2,\dots,N_F$. The constraint (11) can be equivalently written as [9]

$$\frac{1}{N_F}\sum_{n=1}^{N_F}t_{u,n}^k \geq \xi_{u,k}, u = 1,2,\dots,U, k = 1,2,\dots,K,$$
$$P_{u,m}|\boldsymbol{\omega}_{u,m}^k{}^{\text{H}}\boldsymbol{\gamma}_{u,m}|^2 \geq$$
$$(\sum_{l=1}^{U}P_{l,m}|\boldsymbol{\omega}_{u,m}^k{}^{\text{H}}\boldsymbol{\gamma}_{l,m}|^2\bar{\Delta}_{l,k} + ||\boldsymbol{\omega}_{u,m}^k{}^{\text{H}}||^2\sigma_v^2)t_{u,m}^k,$$
$$u = 1,2\dots,U,\forall k = 1,2,\dots,K, m = 1,2,\dots,N_F. \tag{25}$$

Applying (24) to the first part of (25) yields [9]

$$\prod_{n=1}^{N_F}(\frac{t_{u,n}^k}{\Phi_{u,n}^k})^{\Phi_{u,n}^k} \geq N_F\xi_{u,k}, u = 1,2,\dots,U, k = 1,2,\dots,K,$$
$$P_{u,m}|\boldsymbol{\omega}_{u,m}^k{}^{\text{H}}\boldsymbol{\gamma}_{u,m}|^2 \geq$$
$$(\sum_{l=1}^{U}P_{l,m}|\boldsymbol{\omega}_{u,m}^k{}^{\text{H}}\boldsymbol{\gamma}_{l,m}|^2\bar{\Delta}_k + \sigma_v^2|\boldsymbol{\omega}_{u,m}^k|^2)t_{u,m}^k,$$
$$u = 1,2,\dots,U, k = 1,2,\dots,K, m = 1,2,\dots,N_F, \tag{26}$$

which is a valid GP constraint.

Similarly, applying (24) two times to the RHS of (21) yields a constraint (22), where the weights are given in (23) and

$$\theta_{u,pq}^{(1)} = \frac{P_{u,p}P_{u,q}}{\sum_{p',q' \in \mathcal{S}_1}P_{u,p'}P_{u,q'}},$$
$$\theta_{u,pqrs}^{(2)} = \frac{\sqrt{P_{u,p}P_{u,q}P_{u,r}P_{u,s}}}{\sum_{p',q',r',s' \in \mathcal{S}_2}\sqrt{P_{u,p'}P_{u,q'}P_{u,r'}P_{u,s'}}},$$
$$\theta_{u,l}^{(3)} = \frac{P_{u,l}^2}{\sum_{l'=1}^{N_F}P_{u,l'}^2}, \theta_{u,l}^{(4)} = \frac{P_{u,p}P_{u,q}}{\sum_{\substack{p',q'=1 \\ q'>p'}}^{N_F}P_{u,p'}P_{u,q'}}. \tag{27}$$

A successive convex approximation of the convergence and power variance constrained power minimization problem can be written as

$$\begin{aligned}
&\underset{\mathbf{P},\mathbf{t}}{\text{minimize}} && \text{tr}\{\mathbf{P}\} \\
&\text{subject to} && \prod_{n=1}^{N_F}(\frac{t_{u,n}^k}{\Phi_{u,n}^k})^{\Phi_{u,n}^k} \geq N_F\xi_{u,k}, \\
&&& u = 1,2,\dots,U, k = 1,2,\dots,K, \\
&&& P_{u,m}|\boldsymbol{\omega}_{u,m}^k{}^{\text{H}}\boldsymbol{\gamma}_{u,m}|^2 \geq \\
&&& (\sum_{l=1}^{U}P_{l,m}|\boldsymbol{\omega}_{u,m}^k{}^{\text{H}}\boldsymbol{\gamma}_{l,m}|^2\bar{\Delta}_k + \sigma^2|\boldsymbol{\omega}_{u,m}^k|^2)t_{u,m}^k, \\
&&& u = 1,2,\dots,U, k = 1,2,\dots,K, \\
&&& m = 1,2,\dots,N_F, \\
&&& (N_F - 1)(\sum_{l=1}^{N_F}P_{u,l})^2 \leq \mathcal{A}_u(\mathbf{P}_u), u = 1,2,\dots,U, \\
&&& P_{u,m} \geq 0, \quad u = 1,2,\dots,U, m = 1,2,\dots,N_F,
\end{aligned} \tag{28}$$

where $\mathcal{A}_u(\mathbf{P}_u)$ denotes the RHS of (22). The SCA algorithm is summarized in **Algorithm** 1

$$(N_F - 1)(\sum_{l=1}^{N_F} P_{u,l})^2 \leq \left(\frac{\prod_{p,q \in \mathcal{S}_1} \left(\frac{P_{u,p} P_{u,q}}{\theta_{u,pq}^{(1)}} \right)^{\theta_{u,pq}^{(1)}}}{\tau_u^{(1)}} \right)^{\tau_u^{(1)}} \left(\frac{\prod_{p,q,r,s \in \mathcal{S}_2} \left(\frac{\sqrt{P_{u,p} P_{u,q} P_{u,r} P_{u,s}}}{\theta_{u,pqrs}^{(2)}} \right)^{\theta_{u,pqrs}^{(2)}}}{\tau_u^{(2)}} \right)^{\tau_u^{(2)}}$$

$$\times \left(\frac{\sigma^2 N_F^3 \prod_{l=1}^{N_F} \left(\frac{P_{u,l}^2}{\theta_{u,l}^{(3)}} \right)^{\theta_{u,l}^{(3)}}}{\tau_u^{(3)}} \right)^{\tau_u^{(3)}} \left(\frac{2\sigma_s^2 N_F^3 \prod_{\substack{p,q=1 \\ q>p}}^{N_F} \left(\frac{P_{u,p} P_{u,q}}{\theta_{u,pq}^{(4)}} \right)^{\theta_{u,pq}^{(4)}}}{\tau_u^{(4)}} \right)^{\tau_u^{(4)}} \tag{22}$$

$$\tau_u^{(1)} = \frac{\sum_{p,q \in \mathcal{S}_1} P_{u,p} P_{u,q}}{\sum_{p,q \in \mathcal{S}_1} P_{u,p} P_{u,q} + \sum_{p,q,r,s \in \mathcal{S}_2} \sqrt{P_{u,p} P_{u,q} P_{u,r} P_{u,s}} + (\sum_{l=1}^{N_F} P_{u,l})^2 \sigma_s^2 N_F^3}$$

$$\tau_u^{(2)} = \frac{\sum_{p,q,r,s \in \mathcal{S}_2} \sqrt{P_{u,p} P_{u,q} P_{u,r} P_{u,s}}}{\sum_{p,q \in \mathcal{S}_1} P_{u,p} P_{u,q} + \sum_{p,q,r,s \in \mathcal{S}_2} \sqrt{P_{u,p} P_{u,q} P_{u,r} P_{u,s}} + (\sum_{l=1}^{N_F} P_{u,l})^2 \sigma_s^2 N_F^3}$$

$$\tau_3^{(3)} = \frac{\sigma_s^2 N_F^3 \sum_{l=1}^{N_F} P_{u,l}^2}{\sum_{p,q \in \mathcal{S}_1} P_{u,p} P_{u,q} + \sum_{p,q,r,s \in \mathcal{S}_2} \sqrt{P_{u,p} P_{u,q} P_{u,r} P_{u,s}} + (\sum_{l=1}^{N_F} P_{u,l})^2 \sigma_s^2 N_F^3}$$

$$\tau_u^{(4)} = \frac{2\sigma_s^2 N_F^3 \sum_{\substack{p,q=1 \\ q>p}}^{N_F} P_{u,p} P_{u,q}}{\sum_{p,q \in \mathcal{S}_1} P_{u,p} P_{u,q} + \sum_{p,q,r,s \in \mathcal{S}_2} \sqrt{P_{u,p} P_{u,q} P_{u,r} P_{u,s}} + (\sum_{l=1}^{N_F} P_{u,l})^2 \sigma_s^2 N_F^3}. \tag{23}$$

IV. NUMERICAL RESULTS

In this section, numerical results are shown to demonstrate the performance of the proposed algorithm. SCA presented in Section III-C was derived for fixed receiver. The joint optimum can be achieved via alternating optimization [9] which means that the problem is split to the optimization of transmit power for fixed receiver and optimization of receiver for fixed power allocation. Alternating between these two optimization steps converges to a local solution.

The following parameters is used in simulations: $U = 2$, $N_R = 2$, $N_F = 8$, QPSK with Gray mapping, and systematic repeat accumulate (RA) code [14] with a code rate 1/3 and 8 internal iterations are used. The signal-to-noise ratio per receiver antenna averaged over frequency bins is defined by SNR= $\text{tr}\{\mathbf{P}\}/(N_R N_F \sigma_v^2)$. The channel we consider is a quasi-static Rayleigh fading 5-path average equal gain channel.

The complementary cumulative distribution function (CCDF) of PAPR for user 2 for different values of σ_s^2 is depicted in Fig. 3. CCDF is calculated such that 10^5 randomly generated symbol sequences of length N_F for each user is sent over 200 channel realizations. It can be seen from the Fig. 3 that when $\sigma_s^2 = 0.1$ there is not much difference compared to the case where there is no variance constraint. When $\sigma_s^2 = 0.01$ we can obtain a slight PAPR gain with roughly the same SNR compared to the case with no variance constraint. When σ_s^2 is further reduced to 0.001 the PAPR gain is significant. Even though the required SNR to achieve the target MI point increases 1.6 dB, the PAPR gain is much larger than the SNR loss. For example, in the case of no variance constraint we may need to set the maximum transmission power according to 8 dB PAPR while in the case of $\sigma_s^2 = 0.001$ the corresponding PAPR is 3.06 dB. Hence, the gain is 8 dB - 3.06 dB - 1.6 dB = 3.34 dB. Therefore, the coverage of $\sigma_s^2 = 0.001$ precoded transmission is larger compared to the case with no variance constraint.
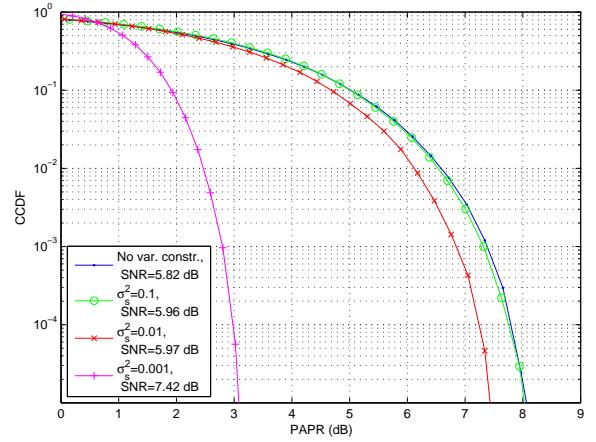

Fig. 3. CCDF of PAPR for user 2. $U = 2$, $N_F = 8$, $N_R = 2$, $\hat{I}_u^{\text{E,target}} = 0.7892$, $u = 1,2$, $\hat{I}_u^{\text{E,target}} = 0.9998$, $\forall u$, $\epsilon_u = 0.01$, $\forall u$, $N_L = 5$.

V. CONCLUSIONS

Transmission power variance constrained power allocation for iterative frequency domain multiuser single input multiple output detector was derived in this paper. The precoding technique takes into account the convergence properties of the iterative receiver while keeping the transmission power variance below the desired threshold. Successive convex approximation was derived for the problem via geometric program. Numerical results demonstrated that the PAPR gain is significantly larger than the SNR loss in the variance constrained precoding technique compared to the case without variance constraint. Hence, the proposed precoding technique increases the coverage of the transmission and is beneficial for power limited cell edge users.

Algorithm 1 Successive convex approximation algorithm.

1: Set $\hat{t}_{u,n}^k = \hat{t}_{u,n}^{k(0)}, \forall u, k, n$ and $\hat{\mathbf{P}}_{u,n} = \hat{\mathbf{P}}_{u,n}^{(0)}, \forall u, n$.
2: **repeat**
3:    Calculate the weights (27) and (23).
4:    Solve Eq. (28).
5:    Update $\hat{t}_{u,n}^k = t_{u,n}^{k(*)}, \forall u, k, n$ and $\hat{\mathbf{P}}_{u,n} = \hat{\mathbf{P}}_{u,n}^{(0)}, \forall u, n$.
6: **until** Convergence.

REFERENCES

[1] F. Pancaldi, G. Vitetta, R. Kalbasi, N. Al-Dhahir, M. Uysal, and H. Mhei-dat, "Single-carrier frequency domain equalization," *Signal Processing Magazine, IEEE*, vol. 25, no. 5, pp. 37–56, 2008.

[2] S. Slimane, "Reducing the peak-to-average power ratio of ofdm sig-nals through precoding," *Vehicular Technology, IEEE Transactions on*, vol. 56, no. 2, pp. 686–695, 2007.

[3] D. Falconer, "Linear precoding of ofdma signals to minimize their instantaneous power variance," *Communications, IEEE Transactions on*, vol. 59, no. 4, pp. 1154–1162, 2011.

[4] C. Yuen and B. Farhang-Boroujeny, "Analysis of the optimum precoder in sc-fdma," *Wireless Communications, IEEE Transactions on*, vol. 11, no. 11, pp. 4096–4107, 2012.

[5] C. Studer and E. Larsson, "Par-aware large-scale multi-user mimo-ofdm downlink," *Selected Areas in Communications, IEEE Journal on*, vol. 31, no. 2, pp. 303–313, 2013.

[6] J. Karjalainen, M. Codreanu, A. Tölli, M. Juntti, and T. Matsumoto, "EXIT chart-based power allocation for iterative frequency domain MIMO detector," *IEEE Trans. Signal Processing*, vol. 59, no. 4, pp. 1624–1641, Apr. 2011.

[7] S. ten Brink, "Convergence behavior of iteratively decoded parallel concatenated codes," *IEEE Trans. Commun.*, vol. 49, no. 10, pp. 1727–1737, Oct. 2001.

[8] V. Tervo, A. Tölli, J. Karjalainen, and T. Matsumoto, "On convergence constraint precoder design for iterative frequency domain multiuser SISO detector," in *Proc. Annual Asilomar Conf. Signals, Syst., Comp.*, Pacific Grove, CA, USA, Nov.4–7 2012, pp. 473–477.

[9] ——, "Convergence constrained multiuser transmitter-receiver optimiza-tion in single carrier FDMA," *IEEE Trans. Signal Processing*, 2013, (under review).

[10] S. Boyd and L. Vandenberghe, *Convex Optimization*.   Cambridge, U.K.: Cambridge Univ. Press, 2004.

[11] M. Chiang, "Nonconvex optimization for communication networks," in *Advances in Applied Mathematics and Global Optimization*, ser. Advances in Mechanics and Mathematics, D. Y. Gao and H. D. Sherali, Eds.   Springer US, 2009, vol. 17, pp. 137–196. [Online]. Available: http://dx.doi.org/10.1007/978-0-387-75714-8_5

[12] V. Tervo, A. Tölli, J. Karjalainen, and T. Matsumoto, "PAPR constrained power allocation for iterative frequency domain multiuser SIMO detec-tor," in *Proc. IEEE Int. Conf. Commun.*, Sydney, Australia, Jun.10–14 2014, pp. 1–6 (submitted).

[13] J. Karjalainen, "Broadband single carrier multi-antenna communications with frequency domain turbo equalization," Ph.D. dissertation, University of Oulu, Oulu, Finland, 2011. [Online]. Available: http://herkules.oulu.fi/isbn9789514295027/isbn9789514295027.pdf

[14] D. Divsalar, H. Jin, and R. J. McEliece, "Coding theorems for 'turbo-like' codes," in *Proc. Annual Allerton Conf. Commun., Contr., Comput-ing*, Urbana, Illinois, USA, Sep.23–25 1998, pp. 201–210.